Available online at www.sciencedirect.com
SCIENCE DIRECT®
Brain and Cognition 50 (2002) 396–413
Brain and Cognition
www.academicpress.com

Diffusion-tensor imaging of cognitive performance

Michael Moseley,[a,*] Roland Bammer,[a] and Judy Illes[a,b]

[a] *Department of Radiology, 1201 Welch Road, Lucas MR Center, Stanford University School of Medicine, Stanford, CA 94305-5488, USA*
[b] *Department of Medicine, Stanford Center for Biomedical Ethics, Stanford University, Stanford, CA 94305-5488, USA*

Accepted 29 July 2002

Abstract

MR methods have for some years been used to assess cognitive performance. Recently, studies have shown that diffusion-tensor imaging (DTI), which provides noninvasive maps of microscopic structural information of oriented tissue in vivo, is finding utility in studies of cognition in the normal and abnormal aging population. These studies suggest that water proton nonrandom, anisotropic diffusion measured by DTI is highly sensitive to otherwise subtle disease processes not easily seen with conventional MRI tissue contrast mechanisms and raises new issues of the role of MR in assessing cognitive potential.

Keywords: Diffusion-tensor imaging; Diffusion-weighted imaging; MRI; Cognition; Cognitive performance

1. Magnetic resonance imaging

1.1. Introduction

Magnetic resonance imaging (MRI) has been established for nearly two decades as a superior modality for morphological and anatomical imaging. Noteworthy for exceptionally good submillimeter spatial and subsecond temporal resolution, MRI is now demonstrating the potential of tracing the links between morphology, tissue function, metabolism, blood flow, and hemodynamics in both normal and disease states. More recently, functional MRI techniques that can utilize modern MRI technology and equipment to image the intrinsic hemodynamic and metabolic changes that may occur in human cognitive functions such as vision, motor skills, language, and memory have become commonplace. MRI can acquire functional images noninvasively within minutes from an individual in any plane or volume at comparatively high-resolutions and then overlay observed functional centers of activation onto the underlying cerebral anatomy, imaged

* Corresponding author. Fax: +650-723-5795.
E-mail address: moseley@stanford.edu (M. Moseley).

0278-2626/02/$ - see front matter © 2002 Elsevier Science (USA). All rights reserved.
PII: S0278-2626(02)00524-9

with the same MRI scanner during the same patient exam. A large number of clinical MRI scanners, many of which are capable of acquiring high-speed single-shot images, are changing the field of neuroimaging to provide assessments of brain function in addition to the anatomical MR imaging done worldwide today.

The various MR methodologies used to relate MR findings with cognition fall into three broad components; morphological studies performed with high-resolution conventional (T1- or T2-weigthed) MR imaging to correlate lesion or segmented brain volumes (Convit et al., 2001; Desmond, 2002; Gadian, Mishkin, & Vargha-Khadem, 1999; Mungas et al., 2001), MR spectroscopy (MRS) to measure regional metabolic concentrations and ratios in relation to cognition (Hsu, Du, Schuff, & Weiner, 2001; Martin, 2001) and, most recently, functional MR measures of proton hemodynamics, diffusion, and regional blood oxygenation dependence in cognition (Cabeza, 2001; Casey, Giedd, & Thomas, 2000; D'Esposito, 2000; Hammeke, Bellgowan, & Binder, 2000; Horwitz, Friston, & Taylor, 2000; Le Bihan, 1996; Menon, Gati, Goodyear, Luknowsky, & Thomas, 1998; Turner, 2000). Each has been used in countless studies and each has inherent advantages and disadvantages. Since the typical MR exam is one of integration, many studies today combine at least two of the three types of functional exams. Our goal here is to review the history, capabilities and limitations of this imaging modality, and to discuss some of the ethical challenges posed by the state-of-the-art.

1.2. The advent of functional MRI: fMRI

One of the more exciting recent developments in magnetic resonance imaging has been the noninvasive visualization of human brain function. Previously the exclusive domain of the technology of Positron Emission Tomography (PET), an important subset of "functional" MRI (fMRI) is now capable of mapping functional regions of the human cortex in real time during specific task activation. This is achieved using magnetic susceptibility image contrast and the fact that deoxyhemoglobin in intact erythrocytes is paramagnetic (interacts with the magnetic field) whereas oxyhemoglobin is not. Increases in the local CBF due to activation result in a decrease in the magnetic susceptibility and increases in the local T2 and T2* due to the inflow of oxygenated blood. This increase or decrease in signal intensity in T2* weighted images is termed Blood Oxygenation Level Dependent (BOLD) imaging (Ogawa, Lee, Kay, & Tank, 1990). Although these techniques do not measure tissue perfusion directly, they potentially can contribute significantly to an understanding of organ metabolism by the quantification of oxygen utilization, as well as through tissue response to various therapeutic interventions. Because more than 70% of the brain's blood lies within the capillaries and small venules, the measurement of magnetic susceptibility T2* signal loss predominantly reflects the regional deoxygenation state of the venous system.

Given the diverse potential of MR to provide noninvasive morphological, metabolic, and functional maps of the brain, there is a growing interest in the microstructural and functional characteristics of brain networks, which often form the basis of current etiological concepts. fMRI uses BOLD measures for identifying cortical and subcortical activation has grown significantly over the last decade. Over the same timecourse but to a much smaller degree, DTI, which reveals the course and structural integrity of white matter projections, has developed into a potent technique (Basser, Mattiello, & LeBihan, 1994; Moseley et al., 1990; Pierpaoli & Basser, 1996; Pierpaoli, Jezzard, Basser, Barnett, & Di Chiro, 1996). Because DTI does not require special motivation or performance, group differences in psychiatry are more easily interpreted in terms of underlying pathology. The combination of both fMRI for cortical activation and DTI for structural connectivity offers a promising vehicle

to further extent our current understanding of mental disorders and to identify populations at risk.

1.3. Water proton diffusion and fMRI

Diffusion ''tensor'' imaging is a powerful technique for the assessment of white matter (WM) structural integrity and connectivity. The movement of water in brain is hindered by the presence of cell membranes, myelin sheaths surrounding axons, and other structures, particularly so in WM tracts where the apparent water diffusion is highly anisotropic, since diffusion parallel to axons and myelin bundles is considerably faster than that perpendicular to the axons. Tensors (a mathematical construct useful for describing multi-dimensional vector systems) are ideal for describing proton diffusion restricted by WM tracts, by indicating the direction and the magnitude of restriction (Basser et al., 1994; Pierpaoli & Basser, 1996; Pierpaoli et al., 1996). This in turn offers an index of directional coherence of fiber tracts or integrity of cellular structure. Based on the diffusion tensor, several quantitative and absolute measures can be determined and mapped, such as the apparent diffusion coefficient (ADC), the degree of anisotropy (e.g., fractional anisotropy, FA) (Basser et al., 1994; Pierpaoli & Basser, 1996; Pierpaoli et al., 1996) and measures of the correlation in orientation between a given pixel and its surrounding neighbors (e.g., the lattice anisotropy, LA) (Pierpaoli & Basser, 1996). Over the past decade, diffusion-weighted imaging (DWI) has become an important image modality in the clinical management of stroke and for investigation of mechanisms of neuronal damage in animal models of cerebral ischemia, and the DWIs or the ADC maps are evaluated routinely.

While DTI is being widely used to demonstrate subtle abnormalities in a variety of diseases including multiple sclerosis and schizophrenia, the extent of information offered by a routine DTI exam extends beyond mean diffusivity measures, such as the magnitude of the ADC, which is often a measure of overall water content, and anisotropy indices, which reflect axonal restrictions and myelin content. DTI measures the amount of nonrandomness (anisotropy) of water diffusion within tissues which is function of the degree to which directionally ordered tissues are either maturing or losing their normal integrity. Much of the early excitement in the use of DTI came from the focus on the focal increases in the diffusion anisotropy in WM that occur during the myelination process, making DTI an essential assessment of brain maturation in children (Neil et al., 1998). Pronounced, age-related increases in WM continue during childhood and adolescence; WM increases its overall volume and becomes more myelinated in a region-specific fashion. We expect that future studies will focus on the concurrent use of experimental behavioral test-batteries, with structural MR as well as fMRI imaging, to study developmental changes in structure–function relationships present and important in cognitive studies.

The advent of in vivo DTI allows the noninvasive, rapid measurement of several unique aspects of the bulk tissue microstructure by determining the translational distances and pathways of water proton motions within the tissue microenvironment. DTI yields a series of quantitative measures that reflects the integrity of WM fiber tracts. While the averaged translational motions of an ensemble of water molecules within the imaged voxel is characterized by Brownian motion, DTI measures the magnitude of this apparent motion (the ADC) along any number of fixed and definable directions, making the ADC sensitive to the pathways (magnitude and direction) of water translation. Thus, when the water molecules are unconstrained, the direction of motion is random and is described over time as an isotropic distribution of path lengths, such as that seen in gray matter. In contrast to random (isotopic) proton motions in gray matter, WM has microstructures which impart boundaries or barriers that hinder the normally random Brownian motion of

water protons. The resulting water diffusion is then mapped as differing diffusion rates along and across these series of barriers resulting in nonrandom (anisotropic) diffusion. The ADC values along and across WM tracts for example can vary by as much as fivefold (Moseley et al., 1990). Because WM tracts are highly organized as macrostructured fiber bundles, microscopically ordered axons and microtubules, voxels containing WM show an orientation-dependent ADC which depends on the direction of the specific fiber tracts observed. This orientation effect creates a need for new and unique visualization tools as well as new means of measuring these variables in the context of cognitive performance.

Thus, the degree to which WM is ordered will have a direct and significant impact on the measured ADC values along the various axes. Within an in-plane image, some regions of WM normally should have very high anisotropy, while others should have considerably lower anisotropy even though they are fully volumed, and this probably represents architectural differences in fiber tract organization at the intravoxel level, i.e., intact fibers crossing within a voxel. For example, the normally homogeneously-ordered corpus callosum has a high measured anisotropy, but the crossing WM tracts leading to the frontal lobes exhibit lower anisotropy than the corpus callosum. These studies suggest that neurodegenerative processes that cause changes at the microstructural level, such as the rate of myelination or demyelination, degradation of microtubules, or loss of axonal structure are likely to cause a significant measurable decrease in anisotropy.

The issue of how microstructural elements within WM contribute to the measured proton diffusion anisotropy, Beaulieu and Allen (1994a, 1994b) reported diffusion measurements of water in three central nervous system models, namely the non-myelinated olfactory, and the myelinated trigeminal and optic nerves of the spotted and long-nosed garfish. They found a similar degree of ADC anisotropy (ADC parallel/ADC perpendicular $\sim$3.6) for all three freshly excised nerve types for the olfactory, trigeminal, and optic nerves. The anisotropy of ADC for the nonmyelinated olfactory nerve argues strongly that myelin is not a necessary determinant of diffusion anisotropy in ordered axonal systems (even though it may contribute when present). Garfish nerves treated with vinblastine, to depolymerize microtubules and inhibit fast axonal transport, also exhibit diffusion anisotropy. This early work suggests that myelin is not wholly responsible for the observed anisotropy excluding a significant role for microtubules and fast axonal transport in the anisotropy. They suggest that the many neurofilaments within the myelin sheath may play an important role for the observed orientation effect in WM and nerve fibers. This is significant in that, again, neurodegenerative processes that cause changes at the microstructural level are likely to cause a significant measurable decrease in anisotropy, making the measurement of anisotropy in DTI a valuable adjunct to the cognitive exam, suggesting that changes seen in DTI with cognition may be showing microstructural changes within the local WM involved in that activation pathway.

Given that DTI is sensitive to the microstructure of WM, the influence of WM lesions (WML) on cognitive function is not clear. In community-based MRI studies that have administered mental status tests to subjects who were free of clinically evident neurologic disease, a weak relationship between WML detected by conventional MRI and generalized cognitive function has been reported (Desmond, 2002). In studies that have administered neuropsychological test batteries, a stronger and more specific association has been recognized between WML and deficits in executive function, most likely due to the involvement of frontal–subcortical pathways. The author recommends that future studies be prospective, utilize standardized methods for structural and functional brain imaging, and administer comprehensive neuropsychological assessments to more rigorously investigate the relationship between evolving WML and declining cognitive functions. The evolving role of DTI in unraveling the roles of WM structure, integrity and connectivity in

cognition and mental status has yet to be established, but the first studies are encouraging and noteworthy.

2. Overview of DTI methods

2.1. DTI image acquisition

DTI is usually included in an integrated MR protocol consisting of scout, morphological and functional exams (such as MR spectroscopy or fMRI)-a total protocol that can run up to an hour of scan time. A typical structural imaging protocol would consist of T1-weighted localizers, axial inplane or oblique axial spin-echo (or fast spin-echo) T2-weighted scans. This would be followed by a routine 3D volume scan used for the overlays of the fMRI and (sometimes) the DTI exams. These structural images serve two major purposes; verification of proper slice selection prior to DTI scanning and determination of the sites of fMRI, MRS, and DTI results since voxels may be found to be significantly different on DTI FA maps that are overlaid on these structural images. This makes it possible to not only determine the anatomical locus of differences, but also to quantify those differences in a given anatomical region of interest drawn on the high-resolution structural images.

DTI scans are almost always an axial diffusion-weighted single-shot spin-echo EPI acquired at the same locations as the inplane structural images; the scan time is approximately 3.5 min per average, with 2–4 averages being the norm. The amount of diffusion weighting added to the sequence is determined by the "b" value. Two b values are used, $b = 0$ (no diffusion weighting) and a high b value (of approximately 800–1000 s/mm^2). The high b value is obtained by applying gradients along two axes simultaneously according to the following pattern that yield measurements along six noncollinear directions: $(x, y, z) = [(1, 1, 0), (0, 1, 1), (1, 0, 1), (-1, 1, 0), (0, -1, 1), (1, 0, -1)]$. This is repeated 2–4 times for each slice, with the sign of all the gradients inverted for two of the repetitions. The magnitude images are averaged prior to calculation of the ADCs; this approach eliminates cross-terms with imaging gradients. An additional set of inversion recovery images with cerebrospinal fluid nulling (TI $\sim$ 2100 ms) is also acquired for each slice with $b = 0\,\mathrm{s/mm^2}$. These images are used to unwarp the eddy current effect of the diffusion gradients in the diffusion-weighted images prior to ADC calculations (deCrespigny & Moseley, 1998).

2.2. DTI analysis

The post-acquisition processing of DTI images begins with the unwrapping of eddy currents (deCrespigny & Moseley, 1998; Haselgrove & Moore, 1996). Eddy currents cause geometric image distortions and are introduced by the echo planar diffusion-weighting gradients. These distortions present as shear, magnification, and/or pixel shifts. An acquired set of nulled inversion recovery images is used by several groups to provide a CSF-free outline of the brain needed for segmentation and unwarping (Haselgrove & Moore, 1996; Klingberg et al., 2000). From the averaged and unwarped DWIs, six ADCs are calculated from the six independent scans of the diffusion tensor and the single $b0$ image. The ADC maps acquired represent the tensor of the directionality of the proton diffusion in the oriented WM. From these direction-dependent ADC maps, further processing is needed to fully characterize the WM structure and integrity. From the diffusion tensor in each voxel, one can derive three eigenvectors, defining the direction of the diffusion system, with the corresponding eigenvalues λ_1, λ_2 and λ_3. The three eigenvalues can be then used to construct maps of the relative anisotropy within each voxel and comprise the real power of the DTI exam. There exist a number of different anisotropy measures

constructed from these eigenvalues (Basser et al., 1996; Basser & Pierpaoli, 1998; Pierpaoli et al., 1996), such as the Relative Anisotropy (RA), Lattice Anisotropy (LA), Lattice Index (LI), Anisotropy (AI), and FA. All of these maps show the deviation from random diffusion that the proton experiences within each voxel; of these, the FA is perhaps the commonly used.

Based on the three eigenvalues and the mean eigenvalue (λ), the anisotropy can be measured as the FA, yielding values between 0 (no anisotropy) and 1 (complete ordering) (Basser et al., 1994; Basser & Pierpaoli, 1998; Pierpaoli & Basser, 1996; Pierpaoli et al., 1996). In addition to the effect of cellular integrity, FA depends on how coherent and regular the diffusion is within each voxel being measured. If a voxel contains nonparallel axons, for example, the diffusion within the voxel will be more equal in different directions and thus less anisotropic (Klingberg et al., 2000, 1999; Lim et al., 1999).

Based on the principal eigenvectors, an inter-voxel coherence index, CI (Klingberg et al., 2000; Klingberg, Vaidya, Gabrieli, Moseley, & Hedehus, 1999), can also be calculated. This definition of coherence uses the co-alignment of two vectors in neighboring voxels as measured by the scalar product between the two vectors. The coherence of the fiber tracts in a given reference voxel with the surrounding (8-neighborhood) voxels is then given by the mean of the eight corresponding scalar products. Consequently, CI is also an absolute measure, taking values between 0 (reference voxel orthogonal to all eight neighbors) and 1 (all neighboring voxels perfectly aligned). Fig. 1 below shows CI map of the same slice as the FA map. For display purposes, the CI has been converted to angles and subtracted from 90° to yield high intensity for high degree of coherence. Although CI is more noisy than FA, especially in gray matter, it does contain information that can not be determined from FA alone. Using CI, it is possible to differentiate adjoining WM of similar, high anisotropy but with different primary directions.

2.3. DTI tractography

DTI tractography is becoming one of the most researched areas of DTI (Jones et al., 2002; Lim et al., 1999; Mori et al., 2002; Pajevic, Aldroubi, & Basser, 2002; Pierpaoli et al., 2000). In short, tractography is the science (although many might consider it an art) of using the vector information inherent in the DTI exam to delineate and highlight fiber "connectivity" along voxels, slices and volumes. The potential of defining fiber convergence and divergence is considerable, especially in disease states where the WM is disrupted or displaced (such as deciding if a brain

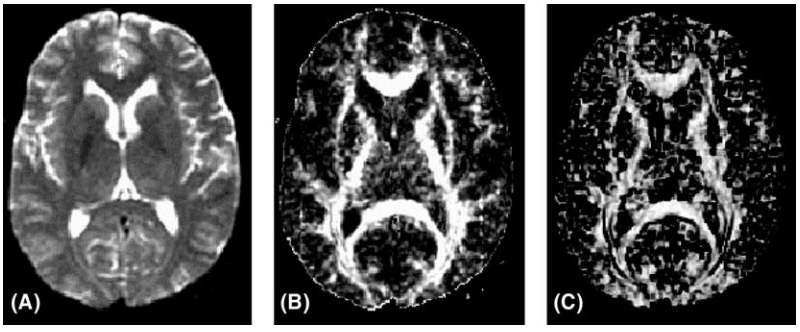

Fig. 1. Three images of a multi-slice diffusion tensor scan. (A) Conventional, T2-weighted image; (B) FA map; white matter is delineated as regions with high intensity (high anisotropy). FA is an absolute, normalized quantity, taking on values between zero (isotropic diffusion) and one, which can be compared directly between subjects or subject groups; (C) CI map of same slice (described above).

tumor has invaded or merely displaced a WM tract). In general, fiber tracking algorithms use a set of conditions to test if the effective diffusion vector such as the principal eigenvalue vector within one voxel could be "connected" to that in the next voxel. If the two vectors are aligned, then we assume that they are connected and that the two voxels describe a part of the WM tract running through them. A tracking algorithm relies on the assumption that the eigenvector at any point in space should be parallel to the tangent of the fiber tract. Interpolation of eigenvector data to subpixel resolution yields a much finer resolution in the fiber maps than in the original data, thus allowing the use of a Runge–Kutta method (for example) for determination of each subsequent point on the fiber tract curve. A user-defined threshold in FA (FA < 0.3) is often used for termination of the tracking algorithm. Tracking is currently being explored as a means of assessing fiber connectivity in normal and disease states in a number of laboratories (see Fig. 2).

A generalized fiber-tracking map is shown in Fig. 3, in which an original vector map is oversampled to a 1024×1024 image size, after which every other point on the map is tested for "connectivity" to the nearest neighbors, within constraints set up by the operator as to the maximum angle of deviations between vectors. This general approach is interesting in that a rough idea of which vectors are "connected" to its neighbors can be assessed by a simple inspection. The value and potential applications of such an approach is being studied using a variety of normal and abnormal cases.

The more specific fiber tracking procedure can be incorporated into an existing 3D visualization program originally developed for analysis of MR angiography data. With the click of a mouse, a point in 3D space is selected as a seed point for the tracking algorithm, projecting both in the forward and backward direction. In

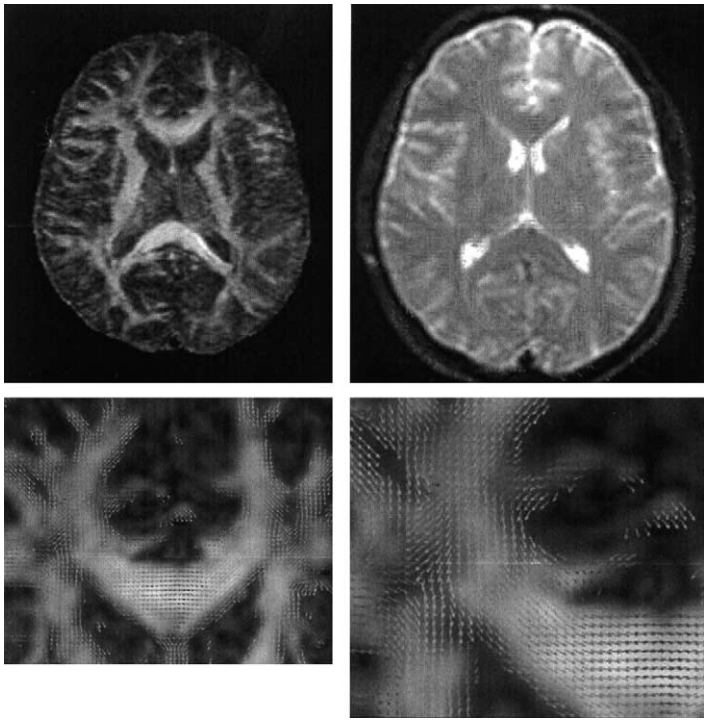

Fig. 2. Upper left: the FA map. Upper right: an illustration of the direction and magnitude of the principal eigenvectors onto the image plane for a section of the genu of the corpus callosum outlined on the T2-weighted image (B0 image). Lower left: vector map. These maps can be further processed to show clearly the extent and direction of the principal eigenvalues. Lower right: zoomed from lower left to show detail.

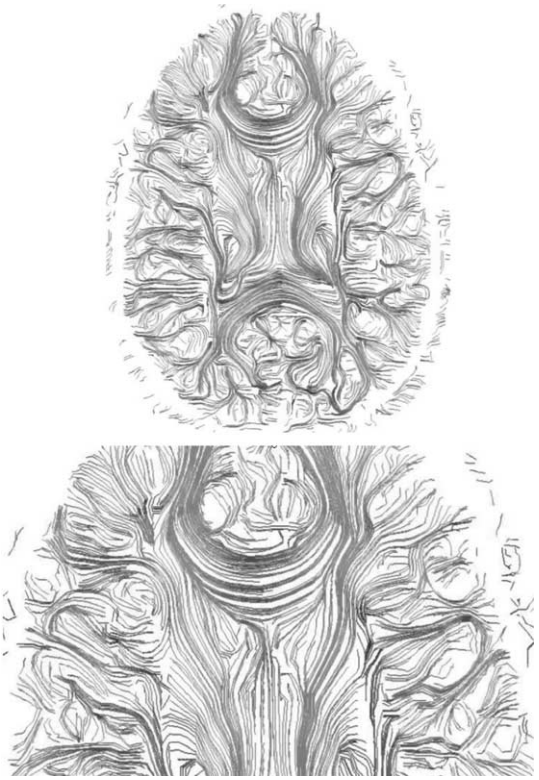

Fig. 3. This map is a representation of the vector map shown above. The genu of the corpus callosum is zoomed below.

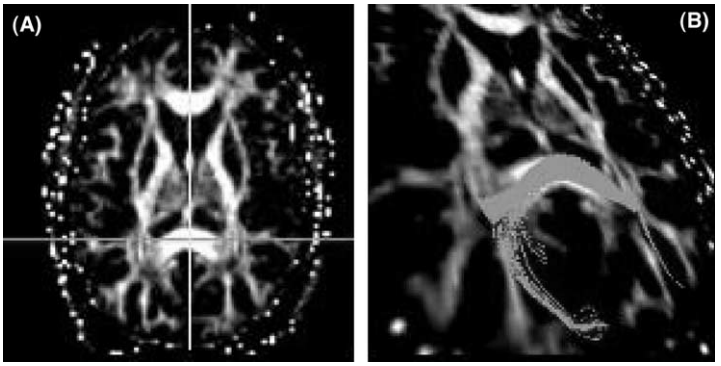

Fig. 4. Axial image of the FA was used to position a seed point for the fiber tracking, shown by the cross-hair on the FA image (A). The resulting tract is overlaid on the same FA image rotated in space to properly display the tract (B).

Fig. 4, an example of tractography shows the result of a fiber tracking with the seed point positioned in the splenium of the corpus callosum. The resulting fiber tract (highlighted) is in agreement with anatomical knowledge of WM fiber pathways.

2.4. Potential pitfalls in DTI

Despite the excitement in the DTI community over the potential of the methodology, there are a number of imaging issues that are critical for the interpretation of DTI findings. In most cases, there is no certain path for what constitutes a correct

versus incorrect interpretation; there is no established gold standard to assess the measurement limits and errors in DTI.

Studies comparing DTI exams across several groups or populations of patients or volunteers have another unique set of considerations. While the use of echo planar MR imaging (EPI) for DTI has proven to be practical for clinical applications because it allows acquisition of multi-slice data in minutes, it suffers from inherent geometric distortions from magnetic field inhomogeneities due to the rapid sampling of the gradient echo train (Andersson, Hutton, Ashburner, Turner, & Friston, 2001; Bammer et al., 2001). While this distortion is tolerable for many clinical applications, it is a serious problem for multiple quantitative studies that are required to map brain diffusion characteristics based on structurally identified, specific anatomic regions of interest, identified from other less-susceptibility prone sequences such as multi-echo spin-echo sequences such as fast spin-echo or FSE (deCrespigny & Moseley, 1998; Haselgrove & Moore, 1996; Tomura et al., 2002). To determine the FA of a given WM structure, it is preferable to identify the structure on nondistorted images with high gray-white tissue conspicuity and co-register these locations on FA images (Lim et al., 1999; Pfefferbaum, Sullivan, Hedehus, Moseley, & Lim, 1999; Pfefferbaum et al., 2000a; Pfefferbaum et al., 2000b; Sullivan et al., 2001). This usually involves the co-registration of rapidly acquired but low-resolution EPI exams with highly detailed conventional MRI images. The issue of geometric distortion now becomes very important when co-registration is required. The Pfefferbaum paper (Pfefferbaum et al., 1999, 2000a, b) implements an approach in which regions of interest defined on dual-echo high-resolution FSE images were co-registered with EPI-based FA maps after the set of EPI images which are obtained without diffusion weighting ($b = 0$) are then spatially warped to the long-echo T_2-weighted FSE images.

Another complicating factor is that intravoxel fiber incoherence (such as fiber crossing or fiber tangles) diminishes the measured FA number within a given voxel (Lim et al., 1999). The conventional six gradient direction scheme models proton diffusion as a symmetrical ellipsoid with three principal axes and cannot adequately handle more complicated patterns of diffusion resulting from fiber paths crossing within a voxel. For this, recent studies have begun analysis of the optimal choice of multiple gradient direction schemes to minimize any intravoxel coherence effects (Wedeen, Reese, Napadow, & Gilbert, 2001; Wiegell, Larsson, & Wedeen, 2000).

Any model can, however, examine the degree to which the diffusion in adjacent voxels has a common principal orientation. This "intervoxel coherence" can be mapped using the orientation of the largest eigenvector of the tensor. This is useful in that it represents a measure of fiber coherence at the voxel level beyond that of the intravoxel measurement. The calculation of intervoxel coherence is based on a determination of the similarity of orientation of adjacent voxels. In other words, if the proton diffusion vector within a given voxel has the same orientation as corresponding vectors from the nearest neighboring voxels, that voxel has a high intervoxel coherence. Because of this property, we anticipate that these measures of intervoxel coherence will become important as work in "fiber-tracking" evolves. In the Pfefferbaum paper (Pfefferbaum et al., 2000a), the investigators implemented a measure of intervoxel coherence, using information from the eigenvector corresponding to the largest eigenvalue (λ_1) from the tensor computations similar to maps of the degree of "alignment" between two neighboring vectors. While not completely independent of FA, images of intervoxel coherence, could conceivably highlight structures, since the coherence should be higher in WM than in gray matter.

Within the fields of aging and cognition, there are the influences of aging on gray and WM atrophy (Guttman, Jolesz, & Kikinis, 1998). Reductions in gray matter

could reduce DTI signals by reducing the substrate of the DTI signal. It is important to examine the relation between DTI measures and measures of gray and WM integrity.

An imaging issue related to atrophy is the transformation of MRI images (both the structural and the DTI images) to a standard brain volume for group comparisons. Such a transformation is necessary to compare whole-brain differences between groups of participants. One approach to this transformation is the normalization module in the Statistical Parametric Mapping software. In SPM, normalization is based on minimizing the sum of squares of the difference between the acquired image and a linear combination of one or more template images. A 12 parameter (consisting of x, y, z translations, rotations, scaling, and shearing) affine transformation is followed by a nonlinear ($7 \times 8 \times 7$ basis) elastic deformation to achieve a closer match to the template image. The template image is based on younger brains, and when trying to normalize elderly brains to this template, problems can occur due to differences in atrophy in the elderly. Investigators have been successful in normalizing elderly brains using SPM, but sometimes extra steps in the process must be considered. These extra steps include: masking the participant's image with a brain mask; truncating the intensity of the participant's image to allow for easier differentiation between CSF, gray, and WM; or re-setting the origin on the images in elderly participants (the origin in SPM is set to the anterior commissure and sometimes this origin needs to be reset in atrophied brains).

2.5. DTI and cognitive function. DTI studies in normal aging and development

Early clinical studies using DTI concentrated on the early and rapid increases in FA seen in neonatal and young childhood development (Neil et al., 1998; Paus et al., 2001). Neonates typically show significantly higher ADC values with lower FA numbers compared with adults; these values becomes more adult-like within about 6 months after birth after which there is a marked decrease in the rate of FA increases in most cerebral WM tissues (Nomura et al., 1994). In a very early study, Peled, Gudbjartsson, Westin, Kikinis, and Jolesz (1998) used line-scan diffusion imaging (acquiring slices in three orthogonal diffusion planes) to measure the three orthogonal diffusion ADC values in 24 men and women, varying in ages from 18 to 44. Although not a strict tensor study in that only three orthogonal axes were measured, the investigators found greater orientation alignment in the anterior limb of the internal capsule on the right than on the left hemisphere. More recently, Klingberg et al. (1999) found lower FA in the frontal white matter in seven children (mean age, 10 years) than in five young adults (mean age, 27 years). These studies add to the suggestion that the measured diffusion anisotropy is directly related to the maturation of WM.

Pfefferbaum et al. (2000b) used measured intravoxel FA values as well as intervoxel coherence (CI) values, to provide a qualitative assessment of age-related changes in WM microstructure. They hypothesized that even in regions of fully volumed WM; FA would decline with age in normal, healthy individuals. In contrast to FA, it was unknown whether the intervoxel coherence CI values would show an age-related decline in neurologically healthy individuals. The measured FA values were found to have a significant regional variation where differences between each regional pairing was significant and progressed from largest to smallest FA as follows: splenium, genu, parietal pericallosal regions, centrum semiovale, and frontal pericallosal regions. For all seven ROIs, median FA was negatively correlated with age. These correlations were significant in the genu, centrum semiovale, and left and right frontal and parietal pericallosal areas but were not significant in the splenium. They observed significant age-related declines in median FA in anatomically determined volumes of densely packed WM fibers. They also found that the highest FA

was present in the regions with the most homogeneously oriented fibers systems, namely, the genu and splenium of the corpus callosum.

The Pfefferbaum paper concluded that FA, as a measure of intravoxel coherence, reflects the integrity of microstructure, such as myelination, microtubule and microfiber condition and integrity. The opposite effect, that is a decrease in FA, with aging may be indicative of mild demyelination and loss of myelinated axons observed in postmortem MRI as well as in histological studies of normal aging (Scheltens et al., 1995).

In a related study using similar MRI and DTI techniques, Sullivan et al. (2001) measured FA between a group of 31 neuropsychologically normal men versus a group of 18 similar matched women. Averaging five regions of interest chosen in the splenium, genu, parietal pericallosal regions, centrum semiovale, and frontal pericallosal regions, they found no significant gender or regional differences in the adult age ranges of 23–79 years. However, they did find small but statistically significant FA differences between every pair of the identified regions, with men and women showing similar patterns of FA magnitudes. In correlations between WM coherence and age, they found negative correlations between FA with age in both men and women, where FA declined with age, as expected. Both men and women exhibited similar patterns of regional FA differences in WM intravoxel and intervoxel coherence.

This study also made a significant contribution to the future potential of DTI by correlating WM intravoxel coherence measured from FA with neuromotor performance exams using tests of gait and balance in these groups. Surprisingly, scores from a finger tapping test correlated with FA in the splenium and in the parietal pericallosal regions. For both of these regions, FA correlated better with task performance than did age. This paper is significant in that it provides one of the first glimpses of in vivo evidence for age-related microstructural deterioration measured by FA of regional WM coherence in both adult men and women in addition to the idea that measured FA values could correlate with motor tasks.

This study is the first to report significant brain FA relationships with behavior in normal aging, in subjects not marked with discrete observable lesions. They go on to conclude that the integrity of the normal aging brain may be slowly eroded by deterioration of the required conductivity to form routine tasks. This study lays the foundation for further correlations between regional WM microstructure and specific cognitive and motor functions with the long-term goal that DTI may provide unique critical outcome measures for evaluating therapy strategies aimed at improving these age-related functional decreases.

2.6. DTI and cognition in dyslexia

DTI was used by Klingberg et al. (2000) to study myelination and architecture of axons in adults subjects with a history of developmental dyslexia. This study is significant in that reports of patients with brain lesions suggested that impairments in reading, so-called acquired dyslexia, can result from damage to the WM tracts connecting the cortical areas necessary for language comprehension (Geschwind, 1965a, b; Sherwin, Geschwind, & Abramowicz, 1965). Prior to the Klingberg study, there was no evidence of WM disturbance in dyslexics. Klingberg chose to look at WM structure using DTI in adults with and without a history of developmental dyslexia (Klingberg et al., 1999). Compared to control subjects, this group exhibited abnormal diffusion of water, indicating decreased myelination of axons, in left and right temporo-parietal WM. The degree of diffusion abnormality within the left of these two regions was strongly correlated with reading ability.

While these reports correlating measured FA with cognitive ability is intriguing, the microenvironment issues behind the WM structure and association is still

unclear. Klingberg et al., rationalized that defective myelination of axons in the left temporo-parietal region of the brain could disrupt the communication between areas necessary for language comprehension and constitute a neurological basis for reading disabilities. They go on to suggest that the localized differences in anisotropy could, in addition to being determined by myelination, also be due to a difference in the coherence of axons; if all axons within a voxel are parallel to each other the anisotropy is high, but if the axons are randomly oriented, diffusion will be the same in all dimensions and the anisotropy will be low. Although there is currently no technique for specifically estimating coherence within voxels, the coherence between voxels can be measured. The principal direction of diffusion in each voxel was computed in the Klingberg study, however, no significant group difference in coherence was noted ($p > .97$). The anisotropy difference in the temporo-parietal regions could thus not be explained as a difference in coherence of taxons, but presumably reflects a difference only in myelination or in the status or integrity of the intramyelin neurofilament bundles.

Case studies suggest that axonal connections in the left temporo-parietal lobe region contain sagittal oriented fibers connecting association areas within the region, as well as sagittal oriented axons from occipital, inferior parietal, and temporal cortex that project to the frontal cortex (Makris, Worth, & Sorenson, 1997). These fibers projecting to the frontal cortex form the external capsule and the arcuate fasciculus/superior longitudinal fasciculus. By superimposing the voxels in question on images describing the fiber direction in single individual subjects, Klingberg confirmed that the disturbance in WM included (but was not confined to) sagittal oriented fibers, adding anatomical evidence to the association between WM disturbance in the left hemisphere and reading disability, since the demonstrated defect in myelination could directly cause reading disability by disrupting communication between the cortical areas necessary for reading. A consequence of decreased myelination or neurofilament integrity would be a slower conduction of neuronal impulses. In their statements, Klingberg et al. (2000), concluded that the decreased myelination or integrity of temporal-parietal and occipital axons could thus simultaneously account for the deficits in auditory and visual processing in dyslexia.

2.7. DTI and cognitive decline

In a series of baseline studies seeking to establish DTI patterns in normal aging to changes seen in suspected cases of cognitive decline such as Alzheimer's dementia (AD), Stebbins et al. (2001a, 2001b) (see also Urresta et al., 2001) examined frontal-lobe FA in selected regions-of-interest (corrected for atrophic differences) in 10 younger (mean age 29 years) and 10 older (mean age 80 years) right handed healthy participants. Participants were group matched for education and pre-morbid IQ. Both groups were highly and equivalently educated, of intact mental status as indicated by the mini mental status scores and of equivalent estimated intelligence. The groups differed significantly on measures of reaction time, processing speed as measured by the Symbol Digit Modalities Test, and reasoning performance as measured by the Raven's Progressive Matrices Test with older persons scoring worse than the younger. Both processing speed and reasoning abilities appear to be important components to executive and working memory processes; processes adversely affected by aging.

DTI was performed using a diffusion-weighted single-shot spin-echo echo-planar sequence using the anatomical slice prescription from a high-resolution FSE series. The DTI data were processed to provide FA with the group DTI data analyses performed using SPM. Immediately before scanning, each subject's reasoning performance was measured. The investigators found that the frontal FA and other regions was significantly reduced in older compared to younger participants

($p < .0001$). The authors suggested that the less organized diffusion in the aged group's WM and greater organization of the diffusion in the younger group's WM, providing a proxy measure for WM integrity. When the investigators then correlated the measured FA with cognitive skills, the processing speed and reasoning performance were significantly correlated with frontal FA ($p < .0001$) while other cognitive parameters such as mental status, education and pre-morbid IQ did not significantly correlate with frontal FA.

From the Stebbins baseline data from normals (Stebbins et al., 2001a, b), Urresta et al. (2001), from the same group examined alterations in FA in patients presenting with cognitive decline. Participants consisted of 10 healthy older right-handed subjects and 10 patients with a diagnosis of probable AD. In those patients with suspected AD, the measured FA was significantly decreased ($p < .05$) in white matter areas corresponding bilaterally to the frontal lobes, the superior longitudinal fasciculus, and the temporal stem. Compared to the effects of normal aging on WM integrity, these results show a further disease-induced deterioration in the microstructure of frontal and temporal lobe WM, but not in the subcortical WM tracts.

The investigators concluded that decreases in frontal WM microstructural integrity measured by DTI FA values occur in older participants independent of atrophic changes. The correlation with reasoning performance supports a role for frontal WM integrity in this ability.

White matter integrity in AD has also been examined by Rose et al. (2000). In this pioneering study, DTI was used to compare the integrity of several WM fiber tracts in patients with probable Alzheimer's disease. Relative to normal controls, patients with probable Alzheimer's disease showed a highly significant reduction in the integrity of tracts such as the splenium of the corpus callosum, superior longitudinal fasciculus, and cingulum relative to the unchanged pyramidal tracts, as measured by the LI of the diffusion anisotropy. This important finding is consistent with a global cognitive decline in Alzheimer's disease and argues for continued research into DTI techniques such as fiber tracking. Specifically, the LI of the splenium of the corpus callosum of patients with probable Alzheimer's disease was highly significantly less than the LI of aged normal controls for left–right oriented fibers and adjoining anteroposteriorly directed callosal fibers. In those patients with mild to moderate probable Alzheimer's disease as measured by the mini mental state examination score (MMSE) (Basser et al., 1994; Basser & Pierpaoli, 1998; Neil et al., 1998; Pierpaoli et al., 1996; Pierpaoli & Basser, 1996), the LI was significantly less than that in the normal controls. A similar significant reduction was also seen in the LI of the fibers of the superior longitudinal fasciculus in patients with probable Alzheimer's disease when compared with controls. A significant reduction was also found for the LI of the anterior–posterior fibers of the left cingulum in the probable Alzheimer's disease cohort. No differences in anisotropy were seen between the two groups for the vertically directed WMTs of the posterior limb of the internal capsule. There was a significant correlation (.77) between the LI of the splenium of the corpus callosum and the MMSE.

This study shows for the first time significant reductions in the LI of the splenium of the corpus callosum, superior longitudinal fasciculus, and left cingulum in patients with probable Alzheimer's disease. Two previous studies have shown a decrease in the measure of relative anisotropy (Haruo, Hiroaki, & Dai, 1997; Sandson, Felician, & Edelman, 1999) in the WM of patients with probable Alzheimer's disease, but neither report correlated anisotropy loss with WMT orientation.

Rose et al. (2000) note that previous pathological studies of patients with Alzheimer's disease have shown that WM abnormalities, such as loss of oligodendrocytes and axons, together with reactive astrocytosis are often seen in the parietal lobe WM and central WM. They go on to suggest that the axon loss in regions of previously high anisotropy caused the decreases in the LI of that region and that the loss

of callosal connections, due to axonal degeneration, could account for the fall in the observed LI values. However, they did caution that reactive astrocytosis and oligodendrocyte loss could also contribute to the fall in LI values in the splenium, superior longitudinal fasciculus, and cingulum of patients with probable Alzheimer's disease. The correlation between the LI of the splenium and the MMSE suggests that a fall in the LI of the splenium of the corpus callosum is related to a decline in cognitive function of these patients. The compelling hypothesis is that there is a link between a loss in the anisotropy of the association fibers of the WMTs and cognitive dysfunction in other dementing illnesses.

Kantarci et al. (2001) also used DTI to assess cognition in AD to compare the regional diffusivity of water in the brains of normally aging elderly people and patients with mild cognitive impairment (MCI) or Alzheimer disease. In 21 patients with Alzheimer disease, 19 patients with MCI, and 55 normally aging elderly control subjects without evidence of cognitive impairment, they measured the ADC and the anisotropy index (AI) in frontal, parietal, temporal, occipital, anterior, and posterior cingulate WM, and the thalami and hippocampi. The hippocampal ADC was higher in MCI and Alzheimer disease patients than in control subjects. The ADC of the temporal stem and posterior cingulate, occipital, and parietal WM was higher in Alzheimer disease patients than in control subjects. Except for occipital AI, which was lower in MCI patients than in control subjects, there were no differences in AI among the three groups for any of the regions. They concluded that the elevation in hippocampal ADC may reflect early ultrastructural changes in the progression of Alzheimer disease but that in their hands using an AI was not conclusive outside of the occipital lobes.

2.8. DTI in MS and vascular disease

Rovaris et al. (2002) report that DTI analyses were sensitive to the macro- and microscopic MS lesion load with increased specificity to the more destructive aspects of MS pathology than conventional imaging. They performed an exploratory study to assess the magnitude of the correlation between quantities derived from DTI (mean ADC and FA) and measures of cognitive impairment in patients with relapsing-remitting MS (RRMS). Moderate correlations were found between symbol digit modalities test, verbal fluency test, and 10/36 spatial recall test scores with T2 and T1 lesion volumes. In a histogram analysis in which the mean ADC and FA were plotted in whole brain tissue, the normal-appearing brain tissue, the normal-appearing WM and the normal-appearing gray matter, moderate correlations were found between symbol digit modalities test, verbal fluency test and 10/36 spatial recall test scores and the DTI correlates. They concluded that DTI provided quantitative metrics that seem to reflect the severity of language, attention, and memory deficits in patients with RRMS.

O'Sullivan et al. (2001a) observed FA changes in ischemic leukoaraiosis as a consistent concomitant of vascular dementia. Conventional MRI provides little information about underlying WM tract disruption and correlates poorly with cognitive dysfunction. They found however, significant changes in the normal-appearing WM were demonstrated in 30 patients with ischemic leukoaraiosis compared with 17 age-matched control subjects when FA was measured. These changes correlated with executive dysfunction assessed by the Wisconsin Card Sorting Test.

This same group also looked at the effects in normal aging with DTI, correlating measured executive skills (the Trail Making Test) with DTI (O'Sullivan et al., 2001b). While it has been suggested that cortical "disconnection" due to the loss of WM fibers may play an important role, but there has been no direct demonstration of structural disconnection in humans in vivo. They found that diffusion anisotropy, a marker of WM tract integrity, was reduced in the WM of older subjects and fell

linearly with increasing age in the older group. Mean diffusivity was higher in the older group and increased with age. In the older group, anterior mean diffusivity correlated with executive function assessed by the Trail Making Test. They conclude that these findings provide direct evidence that WM tract disruption occurs in normal aging and would be consistent with the cortical disconnection hypothesis of age-related cognitive decline. Maximal changes in anterior WM provide a plausible structural basis for selective loss of executive functions.

3. Conclusions

3.1. DTI and neuroethics

Technical advances in MRI over the past 20 years have created stunning advances in the neuroimaging field, expanding the diagnostic and research potentials. Routine procedures are now available that allow acquisition of reference data, morphological assessment and functional characterization. Morphometric and functional brain exams performed on both normal and abnormal patients are now an integral part of many neuroimaging studies, and these capabilities will undoubtedly expand. Research in the neuroimaging field will continue to increase the amount of information obtained through evolving and expanding post-processing procedures, including the powerful methods being developed in multi-modality image fusion.

There has been a move to encourage brain researchers to share raw data from various neuroimaging exams in a community wide database (Marshall, 2000). The publishing of morphological and fMRI images and raw data of the brain the *Journal of Cognitive Neuroscience*, for example, has angered some researchers concerned about the possible misuse of these cognition-sensitive exams, potentially compromising the privacy of research subjects, despite that fact that such a database would be useful for combining results from different studies.

Another potential ramification in assessing cognition potential lies in the definition of cognitive impairment—What constitutes cognitive impairment on the basis of neuroimaging data? How should the concept of cognitive impairment based on either blood oxygenation or microstructural change, or both, be best presented to the patient and the family? Despite the lack of curative treatments, there are compelling reasons why early recognition of Alzheimer's disease, for example, may offer benefits; early diagnosis may offer opportunities to enhance patient safety, allow families to plan for the future, and initiate the best treatment before more substantial neuronal loss occurs. However, failure to recognize the existence or importance of cognitive and functional changes, and/or misperceptions regarding diagnostic requirements and treatment capabilities can be disastrous. False positives can be equally devastating, although it is safe to say that many more studies are needed to address the complex issues of assessing false positives and negatives.

There are also significant ethical questions that surround the concept of informed consent, particularly in patients with neuropsychiatric disorders. With the demonstrated power of the noninvasive MR exam to assess cognitive performance and potential, there is a strong risk of violation of individual privacy. It is not extreme to consider that DTI exam "scores" might be used to admit patients into clinics, homes, or into treatment centers. The DTI exam might also be used to refer patients to a particular therapy. Similarly, DTI could conceivably become a screening option for pre-selecting students or children into educational or special therapy programs. Given the major advantage of DTI over other functional exams in that it does not require any patient or volunteer cooperation, the possibility of finding structural abnormalities at very early ages is wide open. While such abnormalities may predict

eventual cognitive abnormalities later in life and introduces the opportunity for early intervention, the information is also clearly susceptible to misuse.

A tremendous amount of work remains to be done to fully assess the power of DTI and to relate structural patterns to cognitive or motor performance. The first generation of studies suggest that it has enormous potential to do so, and as the DTI exams become faster and have better signal and contrast to noise numbers, we may see DTI be able to sort patients into normal and abnormal populations by scanning alone. These capabilities, and the potential developed beyond these fundamental parameters, may well become the source of significant ethical dilemmas, and legal and societal concern.

Acknowledgments

The authors wish to thank D. Pfefferbaum, E. Sullivan, J. Ford, and G. Stebbins for suggestions, helpful discussions, and the permission to report on recent data. Thanks as well to Phil Letourneau for assistance with the manuscript.

References

Andersson, J. L., Hutton, C., Ashburner, J., Turner, R., & Friston, K. (2001). Modeling geometric deformations in EPI time series. *NeuroImage*, **13**(5), 903–919.

Bammer, R., Keeling, S. L., Augustin, M., Pruessmann, K. P., Wolf, R., Stollberger, R., Hartung, H. P., & Fazekas, F. (2001). Improved diffusion-weighted single-shot echo-planar imaging (EPI) in stroke using sensitivity encoding (SENSE). *Magnetic Resonance in Medicine*, **46**(3), 548–554.

Basser, P. J., Mattiello, J., & LeBihan, D. (1994). MR diffusion tensor spectroscopy and imaging. *Biophysics Journal*, **66**(1), 259–267.

Basser, P. J., & Pierpaoli, C. (1998). A simplified method to measure the diffusion tensor from seven MR images. *Magnetic Resonance in Medicine*, **39**(6), 928–934.

Beaulieu, C., & Allen, P. S. (1994a). Water diffusion in the giantaxon of the squid: Implications for diffusion-weighted MRI of the nervous system. *Magnetic Resonance in Medicine*, **32**(5), 579–583.

Beaulieu, C., & Allen, P. S. (1994b). Determinants of anisotropic water diffusion in nerves. *Magnetic Resonance in Medicine*, **31**(4), 394–400.

Cabeza, R. (2001). Cognitive neuroscience of aging: Contributions of functional neuroimaging. *Scandinavian Journal of Psychology*, **42**(3), 277–286.

Casey, B. J., Giedd, J. N., & Thomas, K. M. (2000). Structural and functional brain development and its relation to cognitive development. *Biological Psychology*, **54**(1–3), 241–257.

Convit, A., Wolf, O. T., de Leon, M. J., Patalinjug, M., Kandil, E., Caraos, C., Scherer, A., Saint Louis, L. A., & Cancro, R. (2001). Volumetric analysis ofthe pre-frontal regions: Findings in aging and schizophrenia. *Psychiatry Research*, **107**(2), 61–73.

deCrespigny, A. J., & Moseley, M. E. (1998). Eddy current induced image warping in diffusion weighted EPI. *Proceedings of the International Society on Magnetic Resonance in Medicine*, 661.

Desmond, D. W. (2002). Cognition and white matter lesions. *Cerebrovascular Diseases*, **13**(Suppl. 2), 53–57.

D'Esposito, M. (2000). Functional neuroimaging of cognition. *Seminars in Neurology*, **20**(4), 487–498.

Gadian, D. G., Mishkin, M., & Vargha-Khadem, F. (1999). Early brain pathology and its relation to cognitive impairment: The role of quantitative magnetic resonance techniques. *Advances in Neurology*, **81,** 307–315.

Geschwind, N. (1965a). Disconnexion syndromes in animals and man. I. *Brain*, **88**(2), 237–294.

Geschwind, N. (1965b). Disconnexion syndromes in animals and man. II. *Brain*, **88**(3), 585–644.

Guttman, C. R. G., Jolesz, F. A., & Kikinis, R., et al. (1998). White matter changes with normal aging. *Neurology*, **50,** 972–978.

Hammeke, T. A., Bellgowan, P. S., & Binder, J. R. (2000). fMRI: Methodology–cognitive function mapping. *Advances in Neurology*, **83,** 221–233.

Haruo, H., Hiroaki, S., & Dai, K., et al. (1997). Increased water diffusion in cerebral white matter in Alzheimer's disease. *Gerontology*, **43,** 343–351.

Haselgrove, J. C., & Moore, J. R. (1996). Correction for distortion of echo-planar images used to calculate the apparent diffusion coefficient. *MRM*, **36,** 960–964.

Horwitz, B., Friston, K. J., & Taylor, J. G. (2000). Neural modeling and functional brain imaging: An overview. *Neural Networks*, **13**(8-9), 829–846.

Hsu, Y. Y., Du, A. T., Schuff, N., & Weiner, M. W. (2001). Magnetic resonance imaging and magnetic resonance spectroscopy in dementias. *Journal of Geriatric Psychiatry and Neurology*, **14**(3), 145–166.

Jones, D. K., Williams, S. C., Gasston, D., Horsfield, M. A., Simmons, A., & Howard, R. (2002). Isotropic resolution diffusion tensor imaging with whole brain acquisition in a clinically acceptable time. *Human Brain Mapping*, **15**(4), 216–230.

Kantarci, K., Jack, C. R., Jr., Xu, Y. C., Campeau, N. G., O'Brien, P. C., Smith, G. E., Ivnik, R. J., Boeve, B. F., Kokmen, E., Tangalos, E. G., & Petersen, R. C. (2001). Mild cognitive impairment and Alzheimer disease: Regional diffusivity of water. *Radiology*, **219**(1), 101–107.

Klingberg, T., Hedehus, M., Temple, E., Salz, T., Gabrieli, J. D., Moseley, M. E., & Poldrack, R. A. (2000). Microstructure of temporo-parietal white matter as a basis for reading ability: Evidence from diffusion tensor magnetic resonance imaging. *Neuron*, **25,** 493–500.

Klingberg, T., Vaidya, C. J., Gabrieli, J. D. E., Moseley, M. E., & Hedehus, M. (1999). Myelination and organization of the frontal white matter in children: A diffusion tensor MRI study. *NeuroReport*, **10,** 2817–2821.

Le Bihan, D. (1996). Functional MRI of the brain principles, applications and limitations. *Journal of Neuroradiology*, **23**(1), 1–5 [Review].

Lim, K. O., Hedehus, M., Moseley, M., de Crespigny, A., Sullivan, E. V., & Pfefferbaum, A. (1999). Compromised white matter tract integrity in schizophrenia inferred from diffusion tensor imaging. *Archives of General Psychiatry*, **56**(4), 367–374.

Makris, N., Worth, A. J., & Sorenson, A. G., et al. (1997). Morphometry of in vivo human white matter association pathways with diffusio-weighted magnetic resonance imaging. *Annals of Neurology*, **42,** 951–962.

Marshall, E. (2000). *Science*, **289**(5484), 1458–1459.

Martin, W. R. (2001). Magnetic resonance imaging and spectroscopy in Parkinson's disease. *Advances in Neurology*, **86,** 197–203.

Menon, R. S., Gati, J. S., Goodyear, B. G., Luknowsky, D. C., & Thomas, C. G. (1998). Spatial and temporal resolution of functional magnetic resonance imaging. *Biochemistry and Cell Biology*, **76**(2–3), 560–571.

Mori, S., Frederiksen, K., van Zijl, P. C., Stieltjes, B., Kraut, M. A., Solaiyappan, M., & Pomper, M. G. (2002). Brain white matter anatomy of tumor patients evaluated with diffusion tensor imaging. *Annals in Neurology*, **51**(3), 377–380.

Moseley, M. E., Cohen, Y., Kucharczyk, J., Mintorovitch, J., Asgari, H. S., Wendland, M. F, Tsuruda, J., & Norman, D. (1990). Diffusion-weighted MR imaging of anisotropic water diffusion in cat central nervous system. *Radiology*, **176**(2), 439–445.

Mungas, D., Jagust, W. J., Reed, B. R., Kramer, J. H., Weiner, M. W., Schuff, N., Norman, D., Mack, W. J., Willis, L., & Chui, H. C. (2001). MRI predictors of cognition in subcortical ischemic vascular disease and Alzheimer's disease. *Neurology*, **57**(12), 2229–2235.

Neil, J. J., Shiran, S. I., McKinstry, R. C., Schefft, G. L., Snyder, A. Z., Almli, C. R., Akbudak, E., Aronovitz, J. A., Miller, J. P., Lee, B. C., & Conturo, T. E. (1998). Normal brain in human newborns: Apparent diffusion coefficient and diffusion anisotropy measured by using diffusion tensor MR imaging. *Radiology*, **209**(1), 57–66.

Nomura, Y., Sakuma, H., Takeda, K., Tagami, T., Okuda, Y., & Nakagawa, T. (1994). Diffusional anisotropy of the human brain assessed with diffusion-weighted MR: Relation with normal brain development and aging. *American Journal of Neuroradiology*, **15,** 231–238.

Ogawa, S., Lee, T. M., Kay, A. R., & Tank, D. W. (1990). Brain magnetic resonance imaging with contrast dependent on blood oxygenation. *Proceedings of the National Academy of Sciences of the United States of America*, **87**(24), 9868–9872.

O'Sullivan, M., Summers, P. E., Jones, D. K., Jarosz, J. M., Williams, S. C., & Markus, H. S. (2001a). Normal-appearing white matter in ischemic leukoaraiosis: A diffusion tensor MRI study. *Neurology*, **57**(12), 2307–2310.

O'Sullivan, M., Jones, D. K., Summers, P. E., Morris, R. G., Williams, S. C., & Markus, H. S. (2001b). Evidence for cortical "disconnection" as a mechanism of age-related cognitive decline. *Neurology*, **57**(4), 632–638.

Pajevic, S., Aldroubi, A., & Basser, P. J. (2002). A continuous tensor field approximation of discrete DT-MRI data for extracting microstructural and architectural features of tissue. *Journal of Magnetic Resonance*, **154**(1), 85–100.

Paus, T., Collins, D. L., Evans, A. C., Leonard, G., Pike, B., & Zijdenbos, A. (2001). Maturation of white matter in the human brain: A review of magnetic resonance studies. *Brain Research Bulletin*, **54**(3), 255–266.

Peled, S., Gudbjartsson, H., Westin, C.-F., Kikinis, R., & Jolesz, F. A. (1998). Magnetic resonance imaging shows orientation and asymmetry of white matter fiber tracts. *Brain Research*, **780,** 27–33.

Pfefferbaum, A., Sullivan, E. V., Hedehus, M., Moseley, M., & Lim, K. O. (1999). Brain gray and white matter transverse relaxation time in schizophrenia. *Psychiatry Research*, **91**(2), 93–100.

Pfefferbaum, A., Sullivan, E. V., Hedehus, M., Adalsteinsson, E., Lim, K. O., & Moseley, M. (2000a). In vivo detection and functional correlates ofwhite matter microstructural disruption in chronic alcoholism. *Alcohol Clinical Experimental Research*, **24**(8), 1214–1221.

Pfefferbaum, A., Sullivan, E. V., Hedehus, M., Lim, K. O., Adalsteinsson, E., & Moseley, M. (2000b). Age-related decline in brain white matter anisotropy measured with spatially corrected echo-planar diffusion tensor imaging. *Magnetic Resonance in Medicine*, **44**(2), 259–268.

Pierpaoli, C., & Basser, P. J. (1996). Toward a quantitative assessment of diffusion anisotropy. *Magnetic Resonance in Medicine*, **36**(6), 893–906.

Pierpaoli, C., Jezzard, P., Basser, P. J., Barnett, A., & Di Chiro, G. (1996). Diffusion tensor MR imaging of the human brain. *Radiology*, **201**(3), 637–648.

Rose, S. E., Chen, F., Chalk, J. B., Zelaya, F. O., Strugnell, W. E., Benson, M., Semple, J., & Doddrell, D. (2000). Loss of connectivity in Alzheimer's disease: An evaluation of white matter tract integrity with colour coded MR diffusion tensor imaging. *Journal of Neurology, Neurosurgery and Psychiatry*, **69,** 528–530.

Rovaris, M., Iannucci, G., Falautano, M., Possa, F., Martinelli, V., Comi, G., & Filippi, M. (2002). Cognitive dysfunction in patients with mildly disabling relapsing-remitting multiple sclerosis: An exploratory study with diffusion tensor MR imaging. *Journal of Neurological Sciences*, **195**(2), 103–109.

Sandson, T., Felician, O., & Edelman, P., et al. (1999). Diffusion-weighted magnetic resonance imaging in Alzheimer's disease. *Dementia and Geriatric Cognitive Disorders*, **10,** 166–171.

Scheltens, P., Barkhof, F., Leys, D., Wolters, E. C., Ravid, R., & Kamphorst, W. (1995). Histopathologic correlates of white matter changes on MRI in Alzheimer's disease and normal aging. *Neurology*, **45,** 883–888.

Sherwin, I., Geschwind, N., & Abramowicz, A. (1965). Language-induced epilepsy. *Transactions of the American Neurological Association*, **90,** 182–188.

Stebbins, G. T., Carillo, M. C., Medina, D., deToledo-Morrell, L., Klingberg, T., Poldrack, R. A., Moseley, M. E., Karni1, O., Wilson, R. S., Bennett, D. A., & Gabrieli, J. D. E. (2001a). Frontal white matter integrity in aging and its role in reasoning performance: A diffusion tensor imaging study. *Society for Neuroscience* [Abstract].

Stebbins, G. T., Poldrack, R. A., Klingberg, T., Carrillo, M. C., Desmond, J. E., Moseley, M. E., Hedehus, M., Wilson, R. S., Karni, O., Bennett, D. A., deToledo-Morrell, L., & Gabrieli, J. D. E. (2001b). Aging effects on white matter integrity and processing speed: A diffusion tensor imaging study. *Neurology*, **56**(Suppl. 3), A374.

Sullivan, E. V., Adalsteinsson, E., Hedehus, M., Ju, C., Moseley, M., Lim, K. O., & Pfefferbaum, A. (2001). Equivalent disruption of regional white matter microstructure in aging healthy men and women. *NeuroReport*, **12**(1), 99–104.

Tomura, N., Kato, K., Takahashi, S., Sashi, R., Izumi, J., Narita, K., & Watarai, J. (2002). Multi-shot echo-planar Flair imaging of brain tumors: Comparison of spin-echo T1-weighted, fast spin-echo T2-weighted, and fast spin-echo Flair imaging. *Computerized Medical Imaging and Graphics*, **26**(2), 65–72.

Turner, R. (2000). fMRI: Methodology–sensorimotor function mapping. *Advances in Neurology*, **83,** 213–220.

Urresta, F., Medina, D., deToledo-Morrell, F., Gabrieli, J. D. E., Klingberg, T., Moseley, M. E., Wilson, R. S., Bennett, J. D., & Stebbins, G. (2001). In vivo detection of white matter changes in Alzheimer's disease with diffusion tensor imaging. *Society for Neuroscience* [Abstract].

Wedeen, V. J., Reese, T. G., Napadow, V. J., & Gilbert, R. J. (2001). Demonstration of primary and secondary muscle fiber architecture of the bovine tongue by diffusion tensor magnetic resonance imaging. *Biophysics Journal*, **80**(2), 1024–1028.

Wiegell, M. R., Larsson, H. B., & Wedeen, V. J. (2000). Fiber crossing inhuman brain depicted with diffusion tensor MR imaging. *Radiology*, **217**(3), 897–903.